HIGH–RESOLUTION RADIOAUTOGRAPHY OF

GALACTOSE–^{3}H ACCUMULATION

IN RINGS OF HAMSTER INTESTINE

CHARLES E. STIRLING and WILLIAM B. KINTER

With the assistance of DANIEL A. MULLEN

From the Department of Physiology, State University of New York Upstate Medical Center, Syracuse, New York 13210

ABSTRACT

Radioautography of water-soluble substances has posed a major technical problem for the past decade. Utilizing silicone-impregnated plastic sections of frozen-dried tissue, a quantitative method was developed for studying distribution of ^{3}H-labeled galactose, mannitol, and phlorizin. The content of a 2-μ band may be measured with an accuracy of $\pm 20\%$ by light microscopy; radioautographs may also be prepared for the electron microscope. Results with intestinal tissue incubated 1–10 min in vitro and, then, frozen rapidly indicate that the first step in galactose absorption is uphill transport into the brush border of the columnar epithelium. Correction of galactose content for the mannitol space in the brush border suggests that the sugar pump is located at the surface of the microvilli. Further evidence for the surface locus of the glucose-galactose pump was obtained with phlorizin (next paper, reference 40). The galactose content of columnar cell cytoplasm always equalled that of microvilli and no transcellular diffusion gradient could be detected; during the first minutes of incubation, however, a gradient did exist between nucleoplasm and cytoplasm. Downhill exit of galactose from columnar cells may have proceeded either directly across basal membranes to adjacent lamina propria or indirectly via open intercellular spaces. Lastly, even in the absence of muscularis, the connective tissue of the lamina propria constituted enough of a diffusion barrier so that it served as a secondary accumulating compartment for galactose under present in vitro conditions.

INTRODUCTION

During active absorption in vitro, sugars of the glucose-galactose class accumulate in the intestinal wall until the tissue content reaches a level many times that in medium bathing the mucosal epithelium. The fact that the columnar epithelial cells, themselves, constitute the primary site of accumulation was first deduced from indirect evidence (29) and then confirmed by microdissection (26), frozen section radioautography (18, 19), and incubation of isolated cells (16, 39). From this fact, most authors have postulated the following sequence of steps for glucose-galactose absorption in the small intestine: sugar molecules enter the columnar cell via an uphill pump located near the brush border, diffuse through the cytoplasm along a transcellular concentration gradient, and exit downhill across a basal barrier into the underlying lamina propria. Under in vivo conditions, capillary circulation rapidly removes sugar from the lamina propria, and the columnar cell content

585

may not attain the high values reported in vitro (5, 37). The recent observation that biopsied cells from a patient with glucose-galactose malabsorption were unable to accumulate galactose (35) highlights the central role of cell accumulation in active absorption.

Data concerning spatial and temporal features of accumulation at the subcellular level are needed to evaluate the individual steps postulated for the absorption process. To obtain such data, we developed a quantitative radioautographic method which permits measurement of tritium-labeled galactose and other water-soluble compounds in a 2-μ band such as the brush border with an accuracy of $\pm 20\%$. The method utilizes silicone-impregnated plastic sections of frozen-dried tissue, and, consequently, radioautographs can be prepared for electron as well as light microscopy. These technical achievements have not been realized previously with water-soluble substances (1, 11, 14, 28, 30, 33, 41), and, hopefully, it will now be possible to apply high-resolution radioautography to many problems involving test substances not incorporated into cell protein. The present report covers the method and results with galactose-^{3}H and mannitol-^{3}H in rings of hamster intestine. Complementary results with phlorizin-^{3}H are presented in another paper (40) and a radioautographic study of biopsy specimens from a patient with glucose-galactose malabsorption is being prepared for publication.

MATERIALS AND METHODS

Rings of Small Intestine

PREPARATION AND INCUBATION: Intestinal tissue was obtained from adult golden hamsters maintained on standard laboratory diet. A given animal was anesthetized with 100% CO_2, its abdomen opened, and the mesentery stripped from the small intestine. During this last procedure, the muscularis was usually lost. The segment of intestine located between points 10 and 30 cm from the pylorus was excised, immersed immediately in iced saline, flushed through, everted over a glass rod, and cut into narrow rings weighing about 50 mg. A number of these rings were incubated 10–20 min at 37°C in 20 ml of Krebs-Henseleit medium (21) modified to contain 2×10^{-3} M Ca^{++} and then transferred to test incubation flasks with 1-2 ml of this medium containing 15% bovine albumin and appropriate concentrations of test compounds. The albumin caused medium to adhere to the tissue during subsequent dissection and helped

to identify the medium in radioautographs; it does not interfere with absorption (19). Test incubation periods ranged from 1 to 10 min. All flasks were equilibrated with 5% CO_2 and O_2 and shaken at 100 cycles/min.

TEST COMPOUNDS: D-galactose-1-^{3}H (50 mc/mmole) served as radioactive substrate for the sugar-absorption studies. Galactose was used exclusively because only a small fraction is metabolized during transport (22). The nontransported alcohol, D-mannitol-1-^{3}H (100 mc/mmole), was used for estimating the extracellular space of the intestinal brush border. Phlorizin-^{3}H, a water-soluble glycoside, was used for testing the dependence of radioautographic grain density on isotope concentration (Fig. 2). Galactose-^{3}H and mannitol-^{3}H were purchased from the New England Nuclear Corp.; phlorizin-^{3}H was synthesized (40).

SCINTILLATION COUNTING: In all experiments, the incubation media were analyzed. For the galactose-^{3}H experiment (Fig. 4) in which counted tissue-to-medium concentration ratios (T/M) were compared with radioautographically determined cell-to-medium ratios (C/M), an additional ring of intestine was removed after each prescribed incubation period, blotted, weighed, and homogenized. Protein-free aliquots of tissue homogenates and media were prepared with Somogyi's Reagent (38) and counted in Butler's liquid scintillation mixture (2). Counting error was less than 3%.

ASSUMED EQUIVALENCE OF CONTENT AND CONCENTRATION: Strictly, counting and radioautographic analysis for labeled solute yield data in the form of content, e.g. moles of sugar per unit volume or weight of cell, and conversion to the concentration in free solution requires additional information concerning, not only water content, but fractional binding of water and solute. However, opposing theories exist concerning the state of intracellular water (13): one view is that all water along with solute is organized on surfaces of cell protein (23); the generally held view is that molecules other than structural protein and lipid are predominantly in free solution. With regard to solute in intestinal cells, Schultz et al. have recently obtained direct evidence that much of the L-alanine accumulated in vitro is osmotically active and, therefore, unbound (36). Kinter and Wilson have reviewed indirect evidence that sugars of the glucose-galactose class are, likewise, accumulated in the unbound state (19). Thus, for the purposes of presentation and interpretation of results in this paper, the following position was taken: on the basis of above evidence, labeled sugar was deemed to be as free and diffusible within cells as in media; for simplicity, cell water also was assumed free; lastly, correction for water content was judged superfluous when comparing
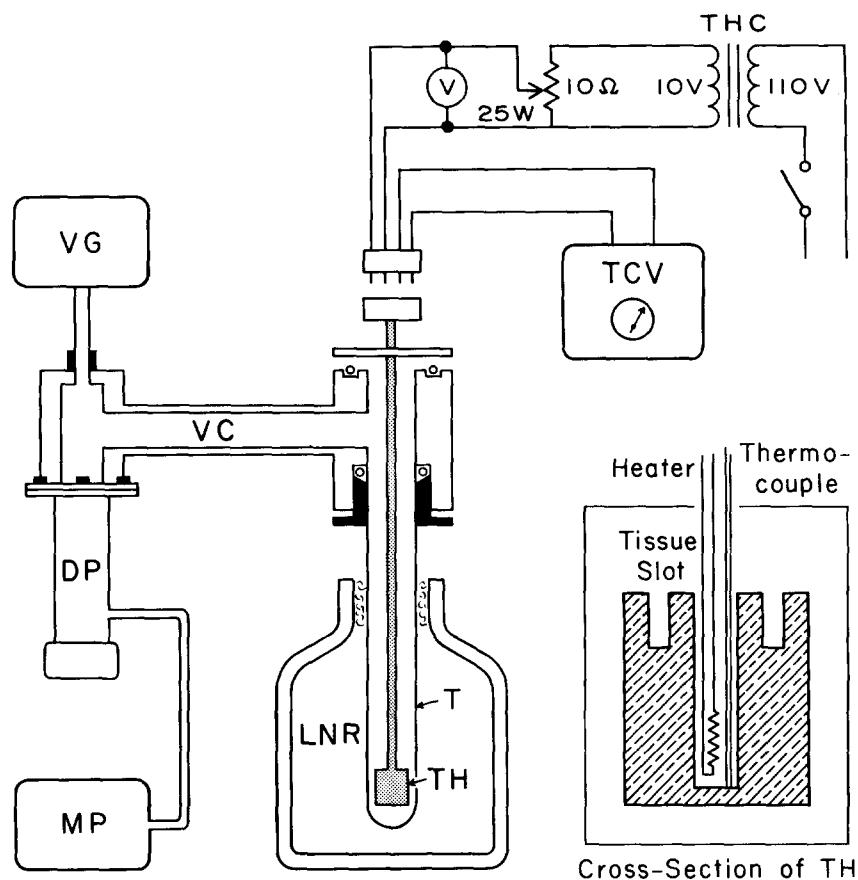
FIGURE 1 Diagram of freeze dryer. The principles of freeze-drying as outlined by Meryman (27) served as a design guide. Briefly, the operation involved loading the slots of the brass tissue holder assembly (*TH*) with frozen tissue and placing the assembly in the trap (*T*) connected to the vacuum chamber (*VC*). The system was evacuated by mechanical (*MP*) and oil diffusion (*DP*) vacuum pumps. When a pressure less than 5×10^{-5} torr was indicated by the vacuum gauge (*VG*), the tissue heater control (*THC*) was adjusted until the tissue reached the desired temperature. This temperature was monitored by a high impedance voltmeter (*TCV*) connected to the calibrated constantan thermocouple in the tissue holder. During drying, water molecules subliming from the heated tissue were trapped by the colder walls of the trap (*T*), a 2-x-24-in. borosilicate glass tube maintained at $-195°C$ by the 25-liter liquid nitrogen refrigerator (*LNR*, Linde Co.). In order to minimize ice artifacts due to recrystallization, the frozen tissue was dried at temperatures below $-40°C$. At $-40°C$ the vapor pressure of ice is less than 0.1 torr; consequently, a high efficiency trapping system was necessary in order to achieve practical drying times (4 days). In the present dryer the position of the tissue in the trap, the low wall temperature, and the high vacuum comprised such a system.

intestinal cells with about 80% water (36) and media with 15% albumin. Hence, as used herein, concentration for both cells and media is numerically equivalent to the measured content in moles per liter.

Frozen-Dried, Plastic-Embedded Tissue

FREEZING: Following a prescribed incubation period, a ring of intestine was removed with a small amount of its incubation medium, placed on a polyethylene pad in a stream of moist 5% CO_2 in O_2, and dissected into 1-2 mg bits. When several bits of tissue had been placed on a prelabeled 3-x-10-mm piece of aluminum foil, they were quickly frozen by plunging the foil into a 100-ml beaker of propane (32) cooled to its melting point, $-184°C$, with liquid nitrogen. Dissection and freezing required about 30 sec. When larger pieces of tissue were frozen (10-100 mg) or when a freezing liquid of higher

melting point was used (dichlorodifluoromethane, mp −160°C), ice-crystal distortion of cell morphology was more evident.

FREEZE-DRYING: After the above procedure was repeated with several rings of intestine, the pieces of foil with adhering tissue were transferred from the propane beaker to a wire sieve supported 1–2 cm above the liquid nitrogen. The beaker was then removed from the liquid nitrogen Dewar and in its place the tissue holder of the freeze dryer (Fig. 1) was cooled to liquid nitrogen temperature. By this time, excess propane had drained away and the pieces of foil with tissue were transferred to the slots in the holder. The holder was then placed in the cold trap of the freeze dryer and the system evacuated (Fig. 1). When a vacuum of 10^{-5} torr (10^{-5} mm Hg) or less was established, the tissue was warmed

Quantitative Radioautography of Water-Soluble Test Compounds

SECTIONING AND EMULSION COATING: Radioautographs for light microscopy were prepared from 1-μ sections cut on an ultratome (LKB) fitted with glass knives. Sections were collected over water, picked up with a stainless steel loop, placed on microscope slides, and dried on a 100°C hot plate. Then a 1-3-μ-thick layer of emulsion was applied by dipping (20): Kodak Type NTB-2 emulsion was melted at 45°C, cooled for 30 min at 30°C, and poured into a disposable polyethylene tube kept in a 30°C water bath. Slides were dipped one at a time, drained, and dried in a dark room maintained at 20°C and 50% relative humidity. The coated slides were exposed in black plastic slide boxes (Clay-Adams) containing 10

TABLE I

Drying Schedule

Temperature (°C)	−195	−70	−50	−30	−20	−10	0	25
Cumulative time (hr)	0–1	50	70	80	90	91	92	93

quickly to −70°C and then gradually, over a period of 4 days, to room temperature; Table I gives a typical drying schedule.

FIXATION AND EMBEDDING: Upon completion of drying, the fragile bits of tissue were transferred to a vacuum desiccator containing a dish of phosphorous pentoxide and 0.1–0.5 g of osmium tetroxide. Air was evacuated from the desiccator and the tissue was fixed in osmium tetroxide vapor for 12 hr. Each tissue sample was then transferred to the side arm of a Thunberg tube (A. H. Thomas Co., Philadelphia) whose lower compartment contained ½ ml of embedding medium. The tubes were evacuated to about 0.2 torr and sealed. After 1 hr, the tubes were evacuated a second time, sealed again, and tilted so that the tissue fell into the embedding medium. The tubes were warmed to 60°C, evacuated a third time, sealed, and placed in a 60°C oven for 12 hr. The impregnated tissue was then removed, blotted, and transferred to polyethylene capsules containing degassed, catalyzed embedding medium. The capsules were placed in a vacuum desiccator, evacuated to about 0.2 torr, and cured for 2 hr at room temperature followed by 36 hr at 48°C. The composition of the embedding medium was by volume: 54% Araldite (Ciba), 45% dodecenyl succinic anhydride, and 1% silicone fluid 200 (Dow-Corning). The medium was catalyzed by 2% benzyldimethylamine. The silicone fluid, immiscible with the other components, was dispersed by 10–20 min of vigorous shaking.

cc of desiccant (Molecular Sieve type 3A, Linde Co., Division of Union Carbide, Tonawanda, N. Y.). Following exposure, usually less than 1 wk, the radioautographs were developed in Kodak D-19 developer for 4 min at 18°C, stopped in distilled water, fixed 4 min in Kodak Rapid Fixer, and washed in several rinses of tap water. The developed radioautographs were then passed through ascending alcohols to xylene and cover slipped. Radioautographs for electron microscopy were prepared by collecting thin sections (gold) on formvar-coated copper grids and coating them with jellied loops of Ilford L-4 emulsion, as described by Caro and Van Tubergen (4), and exposed for about a month.

LEACHING: Movement of water-soluble label into the embedding plastic was not observed. For example, a dried pellet of the albumin incubation medium containing 10^{-7} moles of galactose-^{3}H was suspended in 10 ml of embedding medium and placed in a 60°C oven. After 2 days, the embedding medium was decanted and both the medium and pellet were assayed for radioactivity; the pellet contained better than 99% of the total activity. Furthermore, in the radioautographs no increased activity was detected, over tissue-free areas of plastic, with any test compound studied (see Results). Finally, even after storage of embedded tissue for long periods at room temperature, translocation of test compounds could not be detected, e.g. galactose-^{3}H radioautographs prepared from sections cut within days of embedding
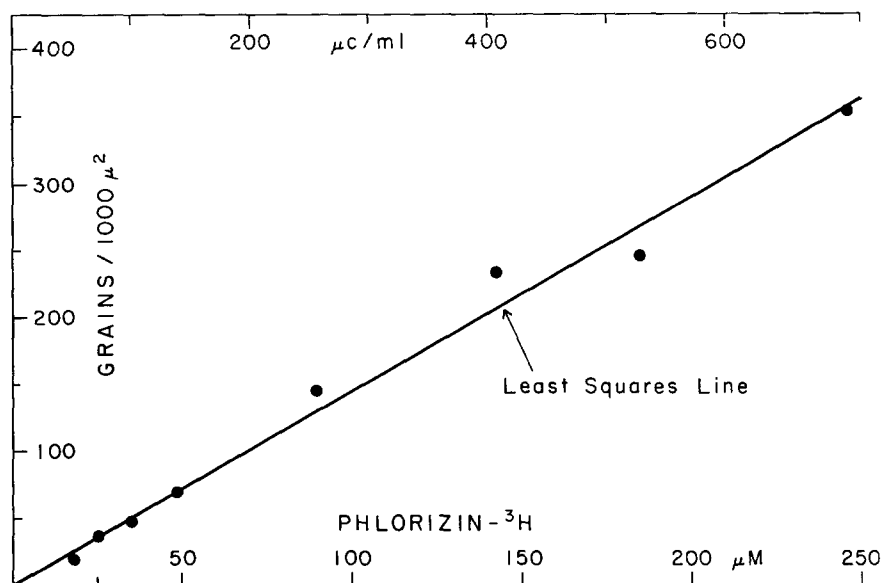
FIGURE 2   Relation between radioautographic grain density and tritium content in sections from a series of eight phlorizin-^{3}H standards. Content is expressed both as μM and as μc/ml in the original standard solutions made with albumin-containing incubation medium. Following rapid freezing, freeze-drying, and plastic embedding of 1–10-μl droplets of each standard, radioautographs were prepared for light microscopy with one batch of NTB-2 emulsion, simultaneous 44-hr exposure, and uniform 4-min development. The present plot consists of mean values for absolute density measurements from three or more sections of each standard (see Table II for detailed data from representative standards).

and 1 year later were similar both by eye and by grain density analysis (Table III).

Conventional fixation and embedding procedures do not render frozen-dried tissue completely water impermeable, and radioautographs produced from sections collected over water or coated with liquid photographic emulsion show gross leaching or diffusion artifacts (11). Evidently, such sections possess water-permeable channels. The present embedding procedure likewise yielded radioautographs with diffusion artifacts when the silicone fluid was omitted from the embedding medium. Although the exact action of this component is not known, it is reasonable to suppose that potential channels for water permeation were wetted or filled by the hydrophobic silicone, thus preventing deep penetration of water after sectioning. Silicone apparently did not prevent surface leaching in the collection bath, since an initial loss of activity always occurred. For example, 1-μ sections from well embedded pellets of galactose-^{3}H and phlorizin-^{3}H incubation media lost about 25% of their radioactivity to the bath water. These sections, like those from any well embedded tissue, yielded radioautographs in which concentration boundaries were sharp and emulsion background was low (see Results). With poorly embedded tissue, e.g. when silicone was omitted, continued loss and

diffusion of labeled compound during drying of sections and coating with liquid emulsion produced dense halos of silver grains over and around the sections. Only radioautographs showing an absence of haloing and having an incubation medium grain density-to-emulsion background grain density ratio of greater than five were accepted for analysis.

Further controls to establish that present procedures permit no selective loss or translocation of labeled test compounds would be difficult to devise. On the other hand, the experimental results in this and a companion study (40) do provide further evidence that the observed radioautographic distribution closely approximates the true tissue distribution at the instant of freezing. First, the diverse radioautographic patterns displayed by the same compound under different experimental conditions and by different compounds (galactose-^{3}H, mannitol-^{3}H, and phlorizin-^{3}H) could hardly have been observed in the presence of selective leaching or diffusion. Second, the many points of quantitative agreement between present radioautographic data and current knowledge of sugar transport leave little doubt concerning the general validity of the method.

PHOTOGRAPHY AND STAINING: Photomicrographs were taken with a Zeiss Universal phase microscope equipped with Planar bright-field and

Neofluor phase objectives and a 4-x-5-inch Polaroid 500 film holder. The number 3 phase disc of the microscope condenser was used to produce dark-field illumination. Dark-field micrographs of the silver grains and all phase-contrast micrographs were made prior to staining; bright-field micrographs were made after staining in a 2% acetone solution of basic fuchsin and again cover slipping. This staining procedure, which did not remove grains, served to differentiate between normal and necrotic cells by staining the latter more lightly (Figs. 5 and 7 a). The electron micrographs were made with an RCA EMU 3D electron microscope operating at 100 kv.

GRAIN DENSITY ANALYSIS: Tissue distribution of test compounds was estimated from light-level radioautographs by counting grains, either with the microscope and an ocular grid or in measured areas of photomicrographs. Irregular areas such as the brush border were outlined with ink on photomicrographs and measured (precision ±4%) with an Ott Plainimeter (F. Weber Co., Philadelphia) prior to counting. The grain density of a particular structure was converted into a content value by comparison with incubation medium in the same radioautograph: structure content = medium content (structure grain density/medium grain density). Validity of this ratio approach depends on density being proportional to content of labeled compound. This fact was verified with a series of phlorizin-^{3}H standards dissolved in albumin incubation medium (Fig. 2). The linear relation between radioautographic grain density and phlorizin-^{3}H concentration also confirms Perry's theoretical prediction (31) that saturation effects, multiple hits on the same silver bromide crystal, are negligible up to about 500 grains/1000 μ^2. Radioautographs with higher grain densities were not used for quantitative analysis.

In analysis of radioautographs, the virtue of the density ratio approach is that random errors arising from differences in section thickness, emulsion sensitivity, development, etc., are minimized when grain density measurements are derived from adjacent areas of a given section. For example, the variability of absolute density values from different sections of representative phlorizin-^{3}H standards (Table II) was much greater than that of the corresponding density ratios. In the derivation of these ratios, individual counts were intentionally limited to 100 grains apiece, the minimum number employed for analysis of a particular structure in a given radioautograph of intestinal tissue. Hence, the random error for ratios from standards (SD up to ±14%) served to establish the general precision of the radioautographic method.

RESOLUTION ERROR: Since concentrations of test compounds in the brush border were of particular interest, it was necessary to determine the additional contribution of resolution error to grain density

TABLE II

Precision (Standard Deviation in Per Cent) of Absolute Grain Density Compared to Density Ratio Measurements in Radioautographs of Sections from Three Phlorizin-^{3}H Standards

Phlorizin conc. and section No.	Absolute density*	Density ratio‡
	grains/1000 μ^2	adjacent 100-grain areas
246 μM		
1	344	1.00
1	342	0.90
2	356	0.89
3	308	0.89
3	322	0.87
4	424	0.93
4	400	0.83
	Mean 357 SD ± 12%	SD ± 12%
185 μM		
1	354	0.88
1	330	0.94
2	167	0.93
2	170	0.75
3	257	0.93
3	204	0.94
	Mean 247 SD ± 33%	SD ± 14%§
49 μM		
1	44	0.95
1	45	0.94
2	111	0.85
2	94	0.88
3	60	0.94
3	52	0.89
	Mean 68 SD ± 41%	SD ± 11%

* Each value based on a count of 200–500 grains corrected for emulsion background; generally, values were obtained from two widely separated areas in the radioautograph of a given section. Most radioautographs analyzed were on different slides and SD for a given standard was expressed as percentage of the mean.

‡ Each ratio based on individual counts of approximately 100 grains apiece from a pair of adjacent areas comprising part or all of the total area counted for the corresponding absolute density value. Grain densities for each pair were arranged so that upon division all ratios were < unity; SD was computed for the difference from unity, i.e. by assuming that the mean for nonarranged ratios would have been unity.

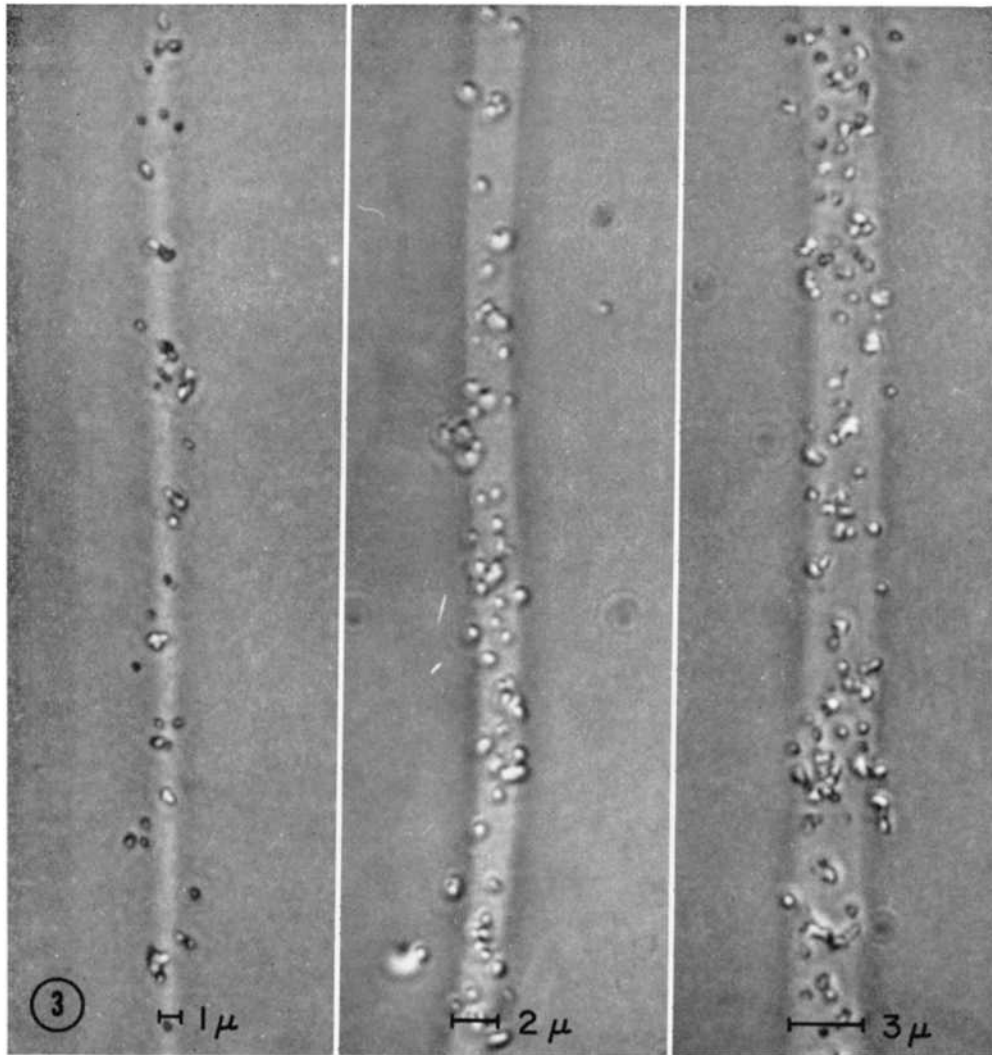§ Highest SD obtained from the eight standards tested (Fig. 2).

FIGURE 3 Radioautographs of uniformly labeled Araldite-³H bands (text). These phase-contrast micrographs were focused at an intermediate plane so that both plastic sections and overlying silver grains could be seen. Note that, although the tritium label is uniformly distributed in the band, the grain distribution varies considerably over distances of a few micra. This variation would be expected from the statistical nature of radioactive decay. × 3,300.

measurements from a narrow band structure. A band source of tritium approximating the dimensions of the brush border was constructed of Araldite-³H (0.9 mc/cc) prepared from succinic-³H acid as described by Hill (15). A large section (3–4 mm²) cut from a block of Araldite-³H was sandwiched between two slabs of methacrylate, re-embedded, trimmed, and sectioned at right angles to the plane of the sandwich. The resulting sections contained a tapered 2-mm-long Araldite-³H band whose width increased from 0.95 μ at the narrow end to 3.0 μ at the wide

end. Radioautographs of the 1-, 2-, and 3-μ regions are presented in Fig. 3. Analysis showed that the percentage of grains lying over the band was 85 ± 4% SD, 97 ± 3% SD, and 100 ± 3% SD, respectively, for these regions. The dimensions of the brush borders analyzed were always between 1 and 3 μ and usually about 2 μ. Thus, even when systematic resolution error (about ±3%) was combined with random precision error for density ratios (±14%) and allowance was made for planimetry error in area measurement (±4%), the over-all ac-

curacy of our radioautographic method at the brush border level was adjudged near ±20%.

RESULTS

Quantitative Radioautography at the Light Microscope Level

SEQUENCE OF GALACTOSE-³H ACCUMULATION: In the experiment illustrated in Fig. 4, whole tissue accumulation by rings of hamster intestine (T/M) increased with time and, if studied longer, probably would have approached asymptotically to a maximum in about 30 min (6). With the present radioautographic method, tissue distribution was investigated during the first 10 min of incubation, the period when galactose content is increasing most rapidly. The micrographs in Fig. 5 were taken at low magnification and demonstrate the distribution in villi after incubation with 1 mM galactose-³H. In bright-field views of stained tissue, the exposed silver grains of the overlying photographic emulsion are not visible; the columnar epithelium and crypts of Lieberkühn are identified by their normal morphological appearance and heavier staining. The amount of subepithelial tissue present depends on the angle and plane of sectioning; the muscularis is absent, having been stripped from the mucosa during preparation. The incubation medium is recognized

by its location at the free or epithelial surface of the villi. In corresponding dark-field micrographs, the exposed silver grains stand out as white dots against a black background, while the tissue is not visible. Since the silver grains correspond to ³H disintegrations, the dark-field views describe the distribution of galactose-³H. Functioning villi appear as white convoluted cones whose brightness indicates the extent of sugar accumulation; some villi with light staining, apparently necrotic epithelial cells (Fig. 7 a), exhibited less ability to concentrate sugar during a given incubation period. After 3 min (Fig. 5 a) the galactose content of villar cores, i.e. lamina propria, was much lower than that of columnar epithelium and about equal to that of medium. However, by 10 min (Fig. 5 b) the cores exhibited a galactose content nearly equal to that of the epithelial cells, indicating secondary movement from cells into lamina propria. Radioautographs of tissue incubated 1 min showed less accumulation than the 3-min tissue (Fig. 4) but, otherwise, were similar. These observations corroborate the well established fact that columnar absorptive cells are the primary site of glucose-galactose accumulation. In fact, at low magnification, the present plastic-section radioautographs appear sharper, but otherwise no different, than earlier frozen-section radioautographs with ¹⁴C-labeled sugars (19).
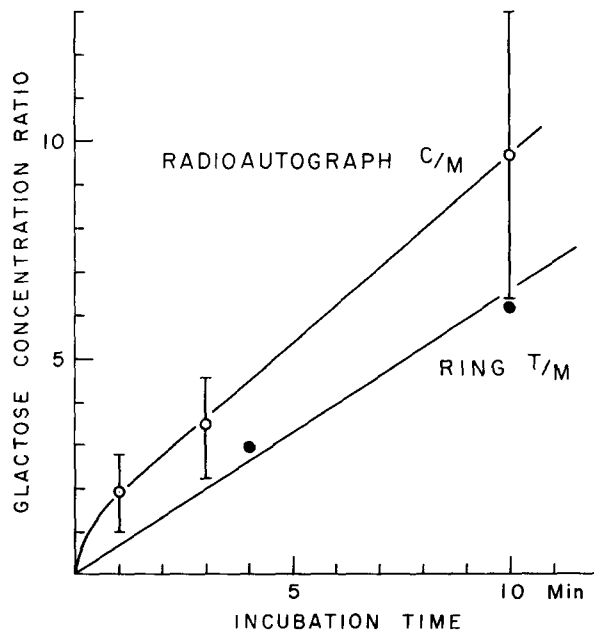
Since the columnar cells are the primary site of

FIGURE 4 Comparison of columnar cell-to-medium (C/M) and whole tissue-to-medium (T/M) concentration ratios from rings of hamster intestine incubated in 1 mM galactose-³H for 1–10 min. Six adjacent rings from one animal (HG-3) were incubated together and, at prescribed times, removed in pairs: one for quantitative radioautography and the other for conventional whole tissue analysis by scintillation counting (Methods). Sample columnar cell measurements are given in Table III; circles with bars give mean ± SD for 10–15 such measurements (total cell) from the radioautographs of two to three of the bits dissected from a given ring. Representative radioautographs from this experiment are shown in Figs. 5–6 and 7 a.
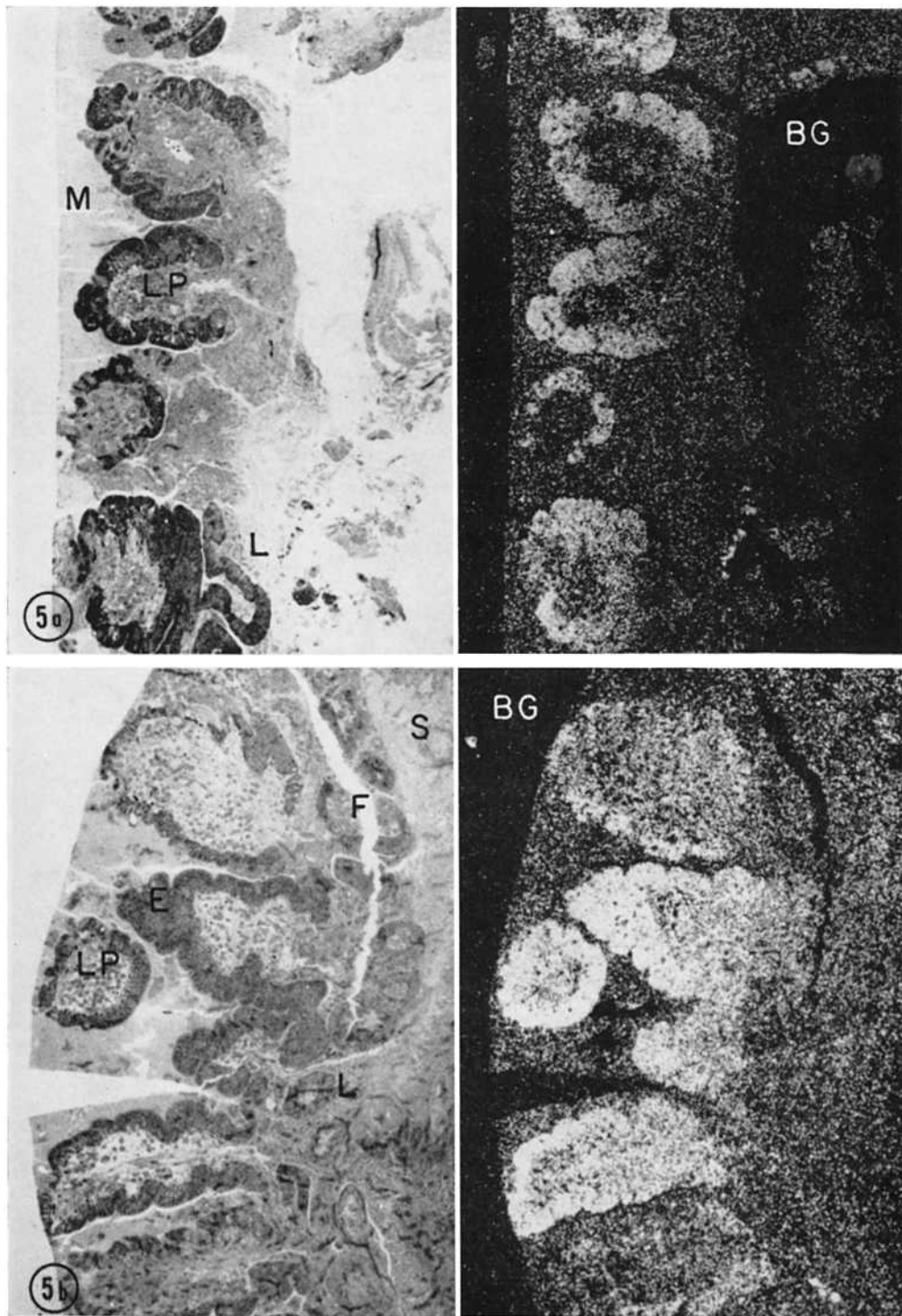
FIGURE 5 Galactose-³H accumulation at the villus level. Photomicrographs on the left are bright-field views of stained sections; those on the right are dark-field views of the overlying radioautographs. They represent intestinal rings (from the same animal) incubated in medium containing 1 mM sugar for (a) 3 min and (b) 10 min. Each section includes about 5 villi cut either in cross-section or obliquely, exposing columnar epithelium (E) and lamina propria (LP). White fissures (F) which interrupt incubation medium (M) and subepithelial tissue (S) are freezing artifacts. In the dark-field views, medium, crypts of Lieberkühn (L) and subepithelial tissue cannot be differentiated, indicating galactose equilibration. The emulsion background (BG) is the region of lowest grain density. Animal HG-3, × 125.

TABLE III

Representative Grain Density Measurements from Individual Radioautographs*

| | | | | Relative galactose-³H content | | | |
| | | | | | Cell | | |
Animal	Tissue incubation	Medium‡	Corrected brush border§	Apical band	Basal band‖	Total¶	Lamina propria
	min						
HG-3							
(Fig. 6 *a*)	1	1.0	3.2	3.4	3.4	3.2	0.9
(Fig. 7 *a*)	3	1.0	4.4	4.1	4.1	3.7	1.4
(Fig. 6 *b*)	10	1.0	7.8	8.2	7.6	8.1	3.6
HG-2**	3	1.0	11.4	11.6	10.5	11.2	4.6
	3	1.0	10.8	11.6	11.6	11.8	3.2
HG-4							
(Fig. 7 *b*)	3	1.0	5.7	9.2	6.4	8.0	2.5

* Micrograph (Fig.) referred to illustrates part or all of the area in which grains were counted; each measurement based on 100 or more grains.

‡ Relative content for grain density of medium taken as unity; actual concentrations from liquid scintillation counting ranged from 1.0 to 1.25 mM galactose.

§ In effect, the microvilli content obtained by correction of measured brush border content for the fractional mannitol-³H space of 0.21 (text):

$$\text{Microvilli} = \frac{\text{brush border} - (0.21 \times \text{medium})}{0.79}$$

‖ Minimal value since no correction was made for open intercellular spaces with low grain densities.

¶ C/M value used in text; includes nuclei and both cytoplasmic bands with no correction for intercellular spaces.

** Second radioautograph was prepared 1 yr later from the same block of plastic-embedded tissue.

galactose accumulation, one would expect cell-to-medium concentration ratios (C/M) to exceed whole tissue-to-medium ratios (T/M). Indeed, this difference was observed (Fig. 4): both the cumulative cell concentration and the net galactose influx (slope) determined from radioautographs were higher, particularly in the first minute, than corresponding quantities derived from conventional whole tissue analyses. One might have expected larger differences since the columnar epithelium represents only a small fraction of the total tissue; however, the lamina propria clearly functioned as a diffusion barrier retarding return of galactose to medium, and the villar cores, in particular, became a secondary accumulating compartment of sizable capacity (Fig. 5). Hence, the total compartment for galactose accumulation was larger than might be predicted on morphological grounds. Cell-to-medium concentration ratios obtained in this study (Fig. 4) are comparable to

those derived from frozen-section radioautographs, e.g. in one animal C/M ranged from 4 to 7 after 10-min incubation with 5.5 mM galactose-¹⁴C (19). An indication of the variability among animals is given in Table III (3-min incubation). Thus, the present method provides quantitative data consistent with both whole tissue and previous radioautographic findings.

DISTRIBUTION IN COLUMNAR EPITHELIUM: The light micrographs in Fig. 6 describe the epithelial distribution of galactose-³H after 1 and 10 min of incubation. At high magnification, the silver grains of the radioautograph stand out as a pattern of black dots against a slightly out-of-focus image of the underlying stained tissue. The incubation medium exhibits a fine reticulation produced by ice-crystal formation during freezing. Frequently, amorphous masses of cell debris, arising from the normal process of columnar cell extrusion, are found in the medium. The brush border is
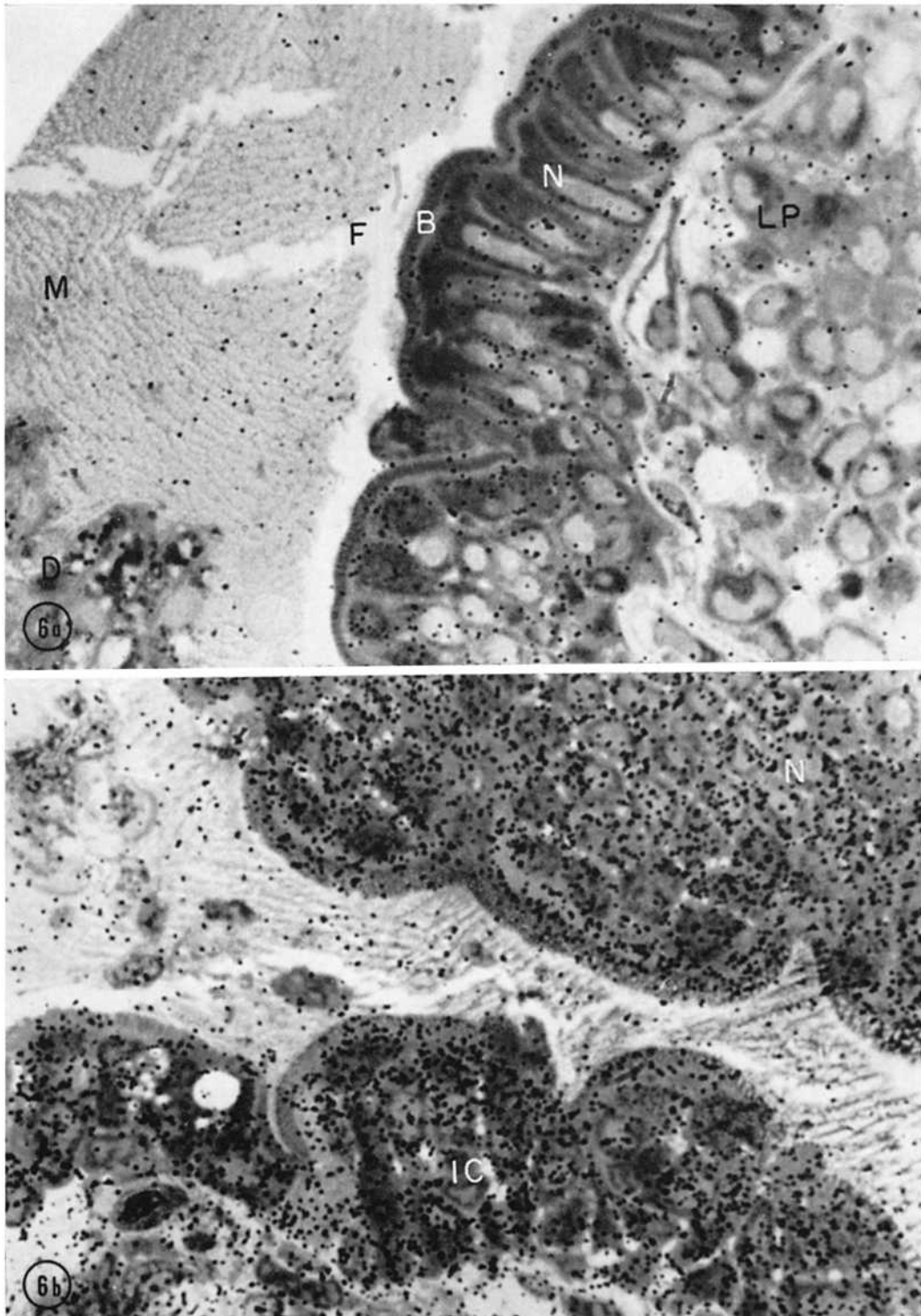
FIGURE 6 Galactose-³H radioautographs at the columnar cell level after (a) 1-min and (b) 10-min incubation in 1 mM sugar. Silver grains appear as black dots. Medium (M) exhibits cell debris (D) and freezing fissures (F); the latter often appear along the brush border (B). Cell nuclei (N) stain lightly in both epithelium and lamina propria (LP). The 10-min tissue shows columnar cells, cut at right angles as well as parallel to their long axes, and some open intercellular spaces (IC). Regions with more prominent spaces were selected for Fig. 7. Animal HG-3, × 1250.

recognized as a 2-μ-wide, somewhat striated band separating medium- and dark-staining cytoplasm. Nuclei stain more lightly than cytoplasm, and intercellular spaces, where open, appear as stain-free areas up to 1 μ wide. The pattern of increasing sugar accumulation with time is clearly evident at high magnification. With 1-min incubation (Fig. 6 a), the grain density over columnar cells showed a distinct step-up from the medium and, after 10 min (Fig. 6 b), the galactose content of both cells and lamina propria was much higher than that of medium.

Although galactose rapidly penetrated brush border membranes, it apparently permeated basal, intercellular and, to some extent, nuclear membranes more slowly. With short incubation times (Figs. 6 a, 7, and 8) the lamina propria, the intercellular spaces, and the central portions of some nuclei were relatively free of silver grains. This was also true for nuclei of connective tissue cells in the lamina propria. After 10 min (Fig. 6 b), galactose of columnar cell nuclei, but not of intercellular spaces or lamina propria, had attained equilibrium with cytoplasmic galactose, which, by then, was rising more slowly (Fig. 4). The sample grain density measurements in Table III also show evidence of slow nuclear equilibration: total cell content, which includes nuclei, only equalled apical cytoplasm after 10 min. The unexpected finding of low galactose content in intercellular spaces at all stages of accumulation was even more evident with higher grain densities; the long exposure radioautograph in Fig. 8 clearly illustrates this important feature of columnar cell absorption. Low content in these spaces suggests either that intercellular membranes are sugar impermeable or that sugar is rapidly swept out of these long channels, perhaps by water flow (Discussion).

Uniformity of galactose distribution within cytoplasm, either along the length of a given cell or in adjacent cells, was another characteristic observed at all stages of accumulation. For example, in any given row of cells (Figs. 6–7) the apical cytoplasm between brush border and nuclei formed an almost continuous band with a surprisingly uniform grain density; local variations reflect the fundamentally random nature of isotopic decay, i.e. the chance disintegration of individual ^{3}H labels (Fig. 3). With higher densities obtained by longer exposure (Fig. 8), chance variation was minimized, emphasizing how little biological variation there was in the

galactose content of adjacent cells. Similarly, the absence of a detectable concentration gradient along the length of columnar cells was established by comparing the apical and the subnuclear, basal band of cytoplasm by eye (Figs. 6–8) and by grain density analysis (Table III). On the other hand, the 2-μ band occupied by brush border always exhibited a detectably lower grain density than the contiguous band of apical cytoplasm. Since it was supected that lower over-all galactose content in the brush border band reflected the presence of incubation media between microvilli, mannitol distribution was investigated.

MANNITOL-^{3}H SPACE IN BRUSH BORDER: Mannitol was selected to estimate the extracellular space of the brush border because it is a nonabsorbed alcohol with a molecular weight comparable to that of galactose. Indeed, even after 3 min of incubation in medium with 0.5 mm mannitol-^{3}H, the intracellular compartment was virtually free of silver grains (Fig. 9). Because incubated rings of intestinal tissue were small (50 mg), some mannitol did diffuse directly from the medium into the lamina propria. The absence of downhill penetration across the brush border in the case of mannitol contrasts strikingly with the uphill accumulation of galactose during the same period of time (Fig. 7). However, a measurable number of grains were present in the brush border band (Fig. 9), indicating that medium did, in fact, penetrate the potential extracellular space between microvilli (Figs. 10–11). If equilibrium is assumed, the fractional mannitol space equalled the brush border-to-medium grain density ratio and averaged 0.21 ± 0.03 SD for 10 measurements on 3-min tissue from a single hamster. This space is consistent with the anatomical value of 0.27 measured from Fawcett's electron micrographs (10).

In turn, when galactose measurements from the brush border were corrected for the average mannitol space (Table III, footnote), the resulting values consistently approximated the apical cytoplasm or total cell content derived from the same radioautographs. For example, corrected brush border-to-total cell galactose averaged 1.13 ± 0.23 SD (P > 0.95 for $\overline{1.13}$ > 1.00) for 12 pairs of measurements on 3-min tissue from animal HG-2 (Table III). Actually, the corrected content represents mostly the microvilli, since brush border minus extracellular space leaves little else. Present resolution, even with electron micrographs

FIGURE 7   Galactose-^{3}H radioautographs of 3-min tissue from two animals (Table III). Both epithelial regions were selected to show many wide open intercellular spaces (*IC*). Note open capillary with red cell (*C*) and group of apparently necrotic columnar cells (*NC*). The cytoplasm, in particular, appears granular and lightly stained; grain density is similar to that of incubation medium, suggesting loss of brush border permeability barrier and rapid equilibration between medium and cytoplasm. (*a*) Animal HG-3, × 1250; (*b*) animal HG-4, × 1600.
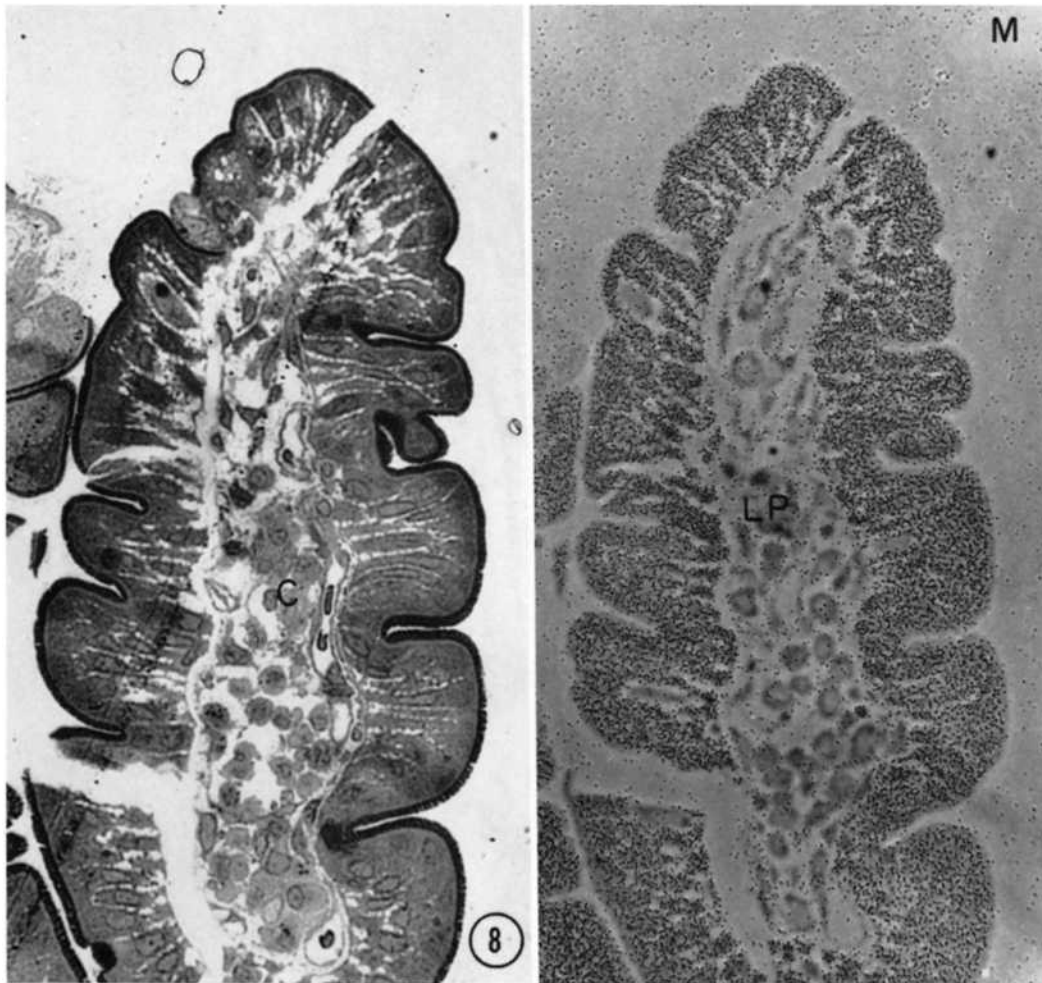
Figure 8 High-grain density radioautograph showing galactose-^{3}H distribution in a single villus, after 3-min incubation. Bright-field view of a nearby stained section (left) shows tissue morphology undisturbed by grains: intercellular spaces, cell nuclei, and capillary with red cells (C). Phase-contrast view of unstained section and overlaying radioautograph (right) shows mostly silver grains and emphasizes that the galactose content of intercellular spaces approximates the low level in medium (M) and lamina propria (LP) rather than the high level in columnar cell cytoplasm (Table III). The high grain density was obtained by exposing the radioautograph for 4 wk; a radioautograph of this tissue with a grain density suitable for analysis is shown in Fig. 7 b. Animal HG-4, $\times$ 500.

(below), does not permit definitive localization of galactose to the surface or the interior of microvilli. However, equality of over-all microvilli content with cell cytoplasm is most easily explained by accumulation within microvilli due to a surface pump. The route and mode of galactose movement from microvilli to lamina propria is more speculative (Discussion).

Preliminary Radioautographs at the Electron Microscope Level

The ultimate aim of our method was to prepare radioautographs for electron microscopy; the micrographs in Figs. 10–12 show results achieved with galactose-^{3}H. Although ice-crystal damage in freeze-dried tissue was not usually apparent at the

FIGURE 9 Mannitol-³H radioautograph showing extracellular space of brush border (text). Grain density in the space is about 20% of that in medium (M); cytoplasmic density is as low as density of the emulsion background (not shown). A remnant of muscularis (MU) is present in this tissue. Animal PB-5, × 1250.

FIGURE 10 Electron micrograph showing brush border accumulation after 3-min incubation in 1 mM galactose-³H. In addition to overlying silver grains (black filaments), the identifiable structures include medium (M) and microvilli and terminal web (TW). Apical cytoplasm from a nearby cell in the same thin section radioautograph is shown in Fig. 11. Animal HG-1, × 17000.

light microscope level, fine reticulation of the cytoplasm was always evident in electron micrographs. Similar damage was observed by Rehbun in freeze-substituted tissue (32). Nevertheless, structures such as microvilli, mitochondria, cell junctions, and intercellular spaces were readily identified. Each radioautographic silver grain in the overlying emulsion was revealed as a twisted
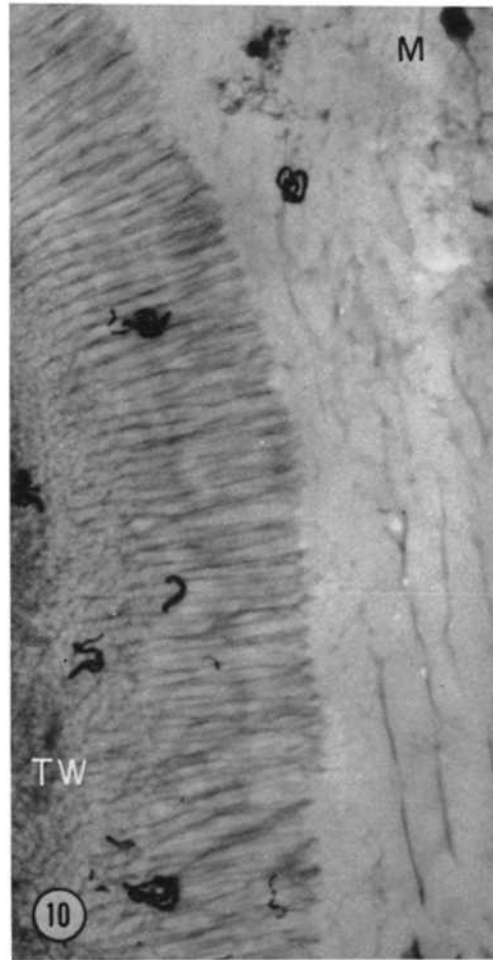
black filament and the resolution with thin sections is such that some part of the filament usually overlies the molecule whose ³H label disintegrated and gave rise to that grain (3, 34). The general distribution of galactose after 3 min of incubation agreed with that found in light-level radioautographs: a large gradient between medium and brush border (Fig. 10); little difference between brush border and cytoplasm (Fig. 11); slightly lower nuclear content (not illustrated); and low
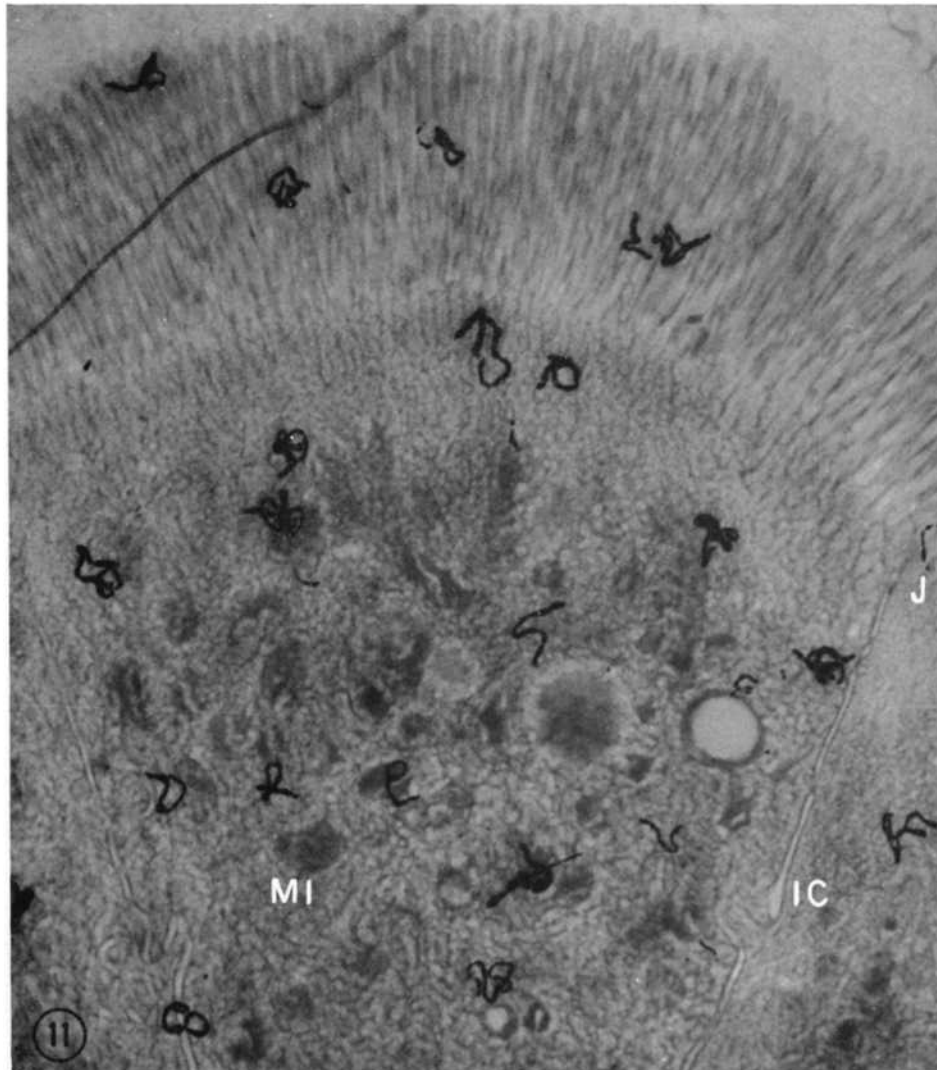
FIGURE 11 Electron micrograph showing 3-min galactose-³H distribution in the apical portion of a columnar cell. Identifiable structures include mitochondria (*MI*) and narrow intercellular spaces (*IC*) extending up to the tight junction (*J*). Incubation medium from this radioautograph is shown in Fig. 10. Animal HG-1, × 19000.

intercellular space content (Fig. 12). Even in electron micrographs, cytoplasmic galactose appeared uniformly distributed and showed no evidence of being associated with any identifiable structure in the several radioautographs prepared from two animals (HG-1 and -2).

Additional information concerning intercellular spaces was also obtained from electron micrographs. First, at cell apices the spaces were too narrow to be resolved in light micrographs. Yet,

it is important to know (Discussion) whether the galactose content remained low or became high in the narrow portion near the terminal web of the brush border. In micrographs like Fig. 11, high content was never detected even next to tight junctions. Second, toward the basal ends of columnar cells in which the spaces were wide, there were many interdigitating cytoplasmic processes overlaid with silver grains (Fig. 12). Thus, some grains which seemed intercellular in light
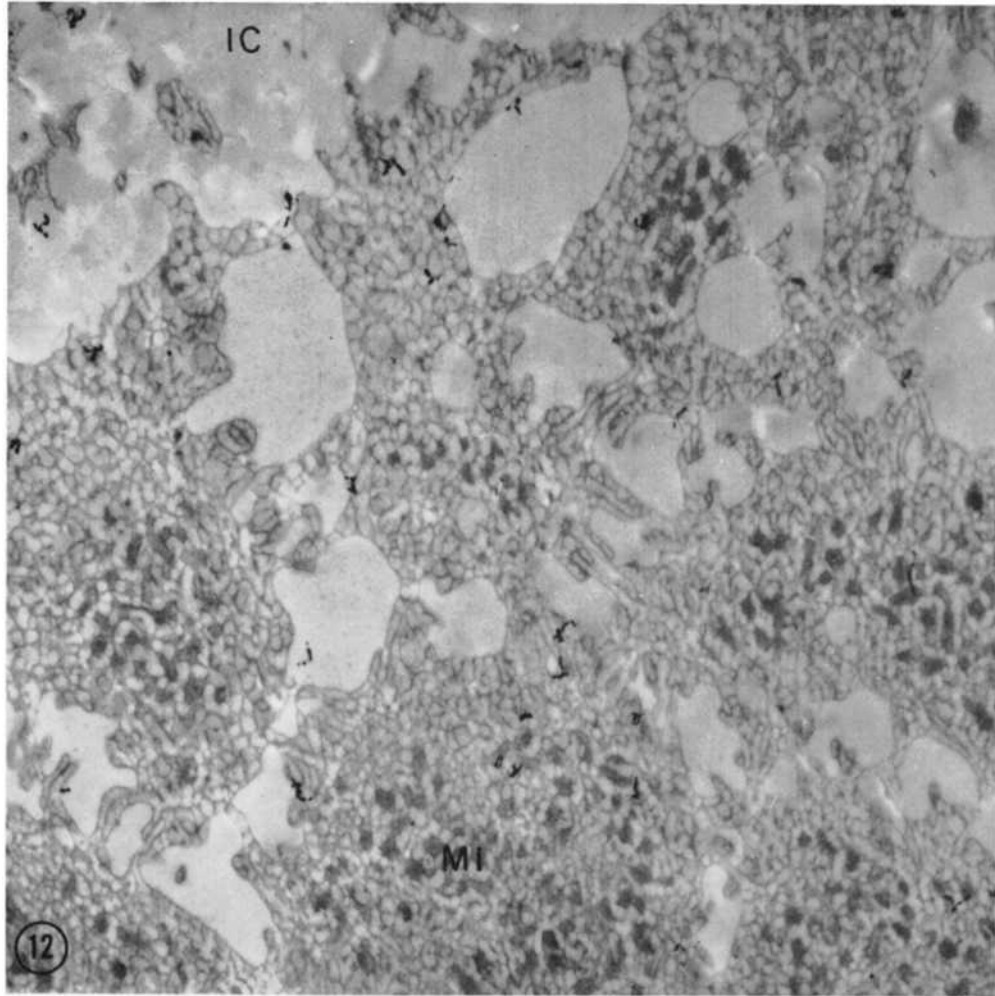
FIGURE 12   Electron micrograph at lower magnification showing basal region of columnar epithelium after 3-min incubation in 1 mM galactose-³H. Plane of section is at right angles to long axis of cells. From several cellular areas with numerous mitochondria (MI) many cytoplasmic processes extend into the wide intercellular spaces (IC). Clearly most silver grains are associated with cytoplasm. Animal HG-2, × 12000.

micrographs (Figs. 6–8) were undoubtedly associated with processes too fine to be resolved and intercellular grain counts were not undertaken at the light level. In the future, we hope to prepare enough electron micrographs to obtain quantitative data on the galactose content of intercellular fluid.

DISCUSSION

The observation that the brush border is the initial site of uphill accumulation supports the

hypothesis that sugars of the glucose-galactose class are transported into epithelial cells by an uphill pump located at the surface of the microvilli (19). Phlorizin-³H radioautographs (see next paper, 40) present stronger evidence for a surface pump. On the other hand, the apparent uniformity of concentration in the microvilli and cytoplasm (Table III) leaves unanswered the question of how galactose transverses the columnar epithelium to the lamina propria. Cytoplasmic diffusion along the length of the cell would require a downhill con-

centration gradient; an estimate of the necessary transcellular gradient was arrived at by assuming that initial flux into the cell via the microvilli pump approximated the steady transcellular flux given by $D\,(Ca - Cb)/L$, where D is the galactose diffusion coefficient, L is the cell length, and Ca and Cb are galactose concentrations in cytoplasm at the apical and basal ends, respectively. Pump flux observed during the first seconds of accumulation was 4 mmole galactose/min × liter cells (Fig. 4, initial C/M slope) or, for a typical columnar cell 20 μ long and 25 μ^2 in cross-section, 1.3×10^{-15} mmole/sec × μ^2. Use of the free diffusion coefficient for galactose, 0.9×10^{-5} cm^2/sec at 37°C, yielded a transcellular concentration difference $(Ca - Cb)$ of 2.9×10^{-2} mM. A gradient of this magnitude superimposed on cytoplasmic concentrations of 3–11 mM galactose (Table III) would amount to less than 1% and be totally undetectable with a radioautographic method good to ±20%. Obviously, the above estimate for gradient is too crude, e.g. application of free diffusion coefficient to cytoplasm, to do more than substantiate our present inability to evaluate the role of transcellular diffusion.

In the absence of a detectable transcellular gradient for galactose, the possibility of non-diffusive movement involving the intercellular spaces merits consideration. It is a fact that during normal sugar absorption there is a simultaneous, sodium chloride-dependent transfer of water from medium to lamina propria (8). In accordance with Curran's general model (7), several authors (9, 17) have proposed the following mechanism for solute-coupled water transport across epithelia: the spaces between cells are maintained in a state of hyper-osmolality by a sodium chloride pump located in the intercellular membrane; water moves osmotically across the brush border, through cytoplasm and into the spaces; this entry of water creates a hydrostatic pressure which both opens the long intercellular channels and causes bulk flow down them, across the highly permeable basement membrane and into the lamina propria. If such a mechanism does function in intestinal epithelium, and clearly intercellular spaces were open (Figs. 6–8, 12), then galactose may exit from columnar cell cytoplasm into these spaces rather than directly into the lamina propria. Certainly, the membrane area bounding the spaces is much greater than the area of cell attachment to the

basement membrane. Moreover, the low galactose concentration within the spaces would provide a large downhill gradient for diffusion across intercellular membranes; the failure to observe a high concentration, even in narrow spaces just under the brush border (Fig. 11), rules out the possibility that galactose, like sodium chloride, was pumped uphill into the spaces. Thus, beyond the microvilli, the primary route of galactose transfer across the columnar epithelium may involve a limited amount of cytoplasm and the long intercellular channels. Much of the transport would be non-diffusive: bulk flow of solution in the spaces and, possibly, solvent drag in the cytoplasm induced by the osmotic flux of water through small cytoplasmic channels. The end result would favor a uniform galactose distribution along the length of a given cell.

The observed uniformity of galactose concentration in cytoplasm of adjacent columnar cells is also of interest. Either the microvilli pump functions uniformly in each cell or galactose equilibrates between cells. Loewenstein (24) has demonstrated intercellular communication in several epithelia; ions and molecules up to large molecular weights move freely from the cytoplasm of one cell to another without leaking to the exterior. If galactose does move rapidly between adjacent cells in intestinal epithelium, the communicating junctions are probably located wherever cytoplasmic processes come into contact across the intercellular space (Figs. 11–12). On the other hand, galactose equilibration with cell nuclei was clearly delayed for some minutes. Whether nuclear membranes constitute a permeability barrier to small ions and molecules has been a point of major controversy in cell physiology (12); the present results, like recent electrical measurements on salivary gland nuclei (25), indicate a significant barrier between cytoplasm and nucleoplasm.

REFERENCES

1. BENDITT, E. P., G. M. MARTIN, and H. PLATTER. 1965. Application of freeze-drying and formaldehyde-vapor fixation to radioautographic localization of soluble amino acids. *In* Symposia of the International Society for Cell Biology. C. P. Leblond, and K. B. Warren, editors. Academic Press Inc., New York. 4:65.

2. BUTLER, F. E. 1961. Determination of tritium in water and urine. *Anal. Chem.* 33:409.

3. CARO, L. G. 1962. High-resolution autoradiography. II. The problem of resolution. *J. Cell Biol.* 15:189.

4. CARO, L. G., and R. P. VAN TUBERGEN. 1962. High-resolution autoradiography. I. Methods. *J. Cell Biol.* 15:173.

5. CRANE, R. K., 1965. Na$^+$-dependent transport in the intestine and other animal tissues. *Federation Proc.* 24:1000.

6. CRANE, R. K., G. FORSTNER, and A. EICHHOLZ. 1965. Studies on the mechanism of the intestinal absorption of sugars X. An effect of Na$^+$ concentration on the apparent Michaelis constants for intestinal sugar transport *in vitro*. *Biochim. Biophys. Acta.* 109:467.

7. CURRAN, P. F. 1960. Na, Cl, and water transport by rat ileum *in vitro*. *J. Gen. Physiol.* 43:1137.

8. CURRAN, P. F. 1965. Ion transport in the intestine and its coupling to other transport processes. *Federation Proc.* 24:993.

9. DIAMOND, J. M., and J. M. TORMEY. 1966. Studies on the structural basis of water transport across epithelial membranes. *Federation Proc.* 25:1458.

10. FAWCETT, D. W. 1962. Physiologically significant specializations of the cell surface. *In* Symposium on The Plasma Membrane. A. P. Fishman, editor. *Circulation.* 26:1105.

11. FITZGERALD, P. J. 1961. "Dry"-mounting autoradiography for intracellular localization of water-soluble compounds in tissue sections. *J. Lab. Invest.* 10:846.

12. GOLDSTEIN, L. 1964. Nucleocytoplasmic relationships. *In* Cytology and Cell Physiology. G. H. Bourne, editor. Academic Press Inc., New York. 3rd Edition. 559.

13. HECHTER, O. 1965. Intracellular water structure and mechanism of cellular transport. *Ann. N. Y. Acad. Sci.* 125:625.

14. HILL, D. K. 1962. The location of creatine phosphate in frog's striated muscle. *J. Physiol. London.* 164:31.

15. HILL, D. K. 1962. Resolving power with tritium autoradiographs. *Nature.* 194:831.

16. HUANG, K. C. 1965. Uptake of L-tyrosine and 3-O-methylglucose by isolated intestinal epithelial cells. *Life Sci.* 4: 1201.

17. KAYE, G. I., H. O. WHEELER, R. T. WHITLOCK, and N. LANE. 1966. Fluid transport in the rabbit gallbladder. *J. Cell Biol.* 30:237.

18. KINTER, W. B. 1961. Autoradiographic study of intestinal transport. *In* Proceedings of the 12th Annual Conference on the Nephrotic Syndrome, Princeton, N. J. J. Metcoff, editor. National Kidney Disease Foundation, N. Y. 59.

19. KINTER, W. B., and T. H. WILSON. 1965. Autoradiographic study of sugar and amino acid absorption by everted sacs of hamster intestine. *J. Cell Biol.* 25 (Pt. 2):19.

20. KOPRIWA, B. M., and C. P. LEBLOND. 1962. Improvements in the coating technique of radioautography. *J. Histochem. Cytochem.* 10: 269.

21. KREBS, H. A., and K. HENSELEIT. 1932. Untersuchungen uber die Harnstoffbildung in Tierkorper. *Z. Physiol. Chem.* 210:33.

22. LANDAU, B. R., and T. H. WILSON. 1959. The role of phosphorylation in glucose absorption from the intestine of golden hamster. *J. Biol. Chem.* 234:749.

23. LING, G. N. 1965. Physiology and anatomy of the cell membrane: the physical state of water in the living cell. *Federation Proc.* 24 (Suppl. 15):S-103.

24. LOEWENSTEIN, W. R. 1966. Permeability of membrane junctions. *Ann. N. Y. Acad. Sci.* 137:441.

25. LOEWENSTEIN, W. R., Y. KANNO, and S. ITO. 1966. Permeability of nuclear membranes. *Ann. N. Y. Acad. Sci.* 137:708.

26. McDOUGAL, D. B., JR., K. D. LITTLE, and R. K. CRANE. 1960. Studies on the mechanism of the intestinal absorption of sugars. IV. Localization of galactose concentrations within the intestinal wall during active transport *in vitro*. *Biochim. Biophys. Acta.* 45:483.

27. MERYMAN, H. T. 1960. Principles of Freeze Drying. *Ann. N. Y. Acad. Sci.* 85:630.

28. MILLER, O. L., G. E. STONE, and D. M. PRESCOTT. 1964. Autoradiography of soluble materials. *J. Cell Biol.* 23:654.

29. NEWEY, H., B. J. PARSONS, and D. H. SMYTH. 1959. The site of action of phlorizin in inhibiting intestinal absorption of glucose. *J. Physiol. London.* 148:83.

30. PELC, S. R., T. C. APPLETON, and M. E. WELTON. 1965. State of light autoradiography. *In* Symposia of the International Society for Cell Biology. C. P. Leblond and K. B. Warren, editors. Academic Press Inc., New York. 4:9.

31. PERRY, R. P. 1964. Quantitative autoradiog-

raphy. *In* Methods in Cell Physiology. D. M. Prescott, editor. Academic Press Inc., New York. 1:305.

32. REBHUN, L. I. 1965. Freeze-substitution: fine structure as a function of water concentration in cells. *Federation Proc.* **24** (Suppl. 15):S-217.

33. ROSSI, G. L., and D. BAIC. 1964. Studies on the site of action of insulin in the penetration of muscle fibers by ^{14}C-D-xylose by means of a general autoradiographic method for localization of diffusible substances. *Exptl. Cell Res.* **36**:169.

34. SALPETER, M. M., and L. BACHMANN. 1965. Assessment of technical steps in electron microscope autoradiography. *In* Symposia of the International Society for Cell Biology. C. P. Leblond and K. B. Warren, editors. Academic Press Inc., New York. 4:23.

35. SCHNEIDER, A. J., W. B. KINTER, and C. E. STIRLING. 1966. Glucose-galactose malabsorption: report of a case with autoradiographic studies of a mucosal biopsy. *New Engl. J. Med.* **274**:305.

36. SCHULTZ, S. G., R. E. FUISZ, and P. F. CURRAN. 1966. Amino acid and sugar transport in rabbit ileum. *J. Gen. Physiol.* **49**:849.

37. SMYTH, D. H. 1965. Water movement across the mammalian gut. *Symp. Soc. Exptl. Biol.* **19**:307.

38. SOMOGYI, M. 1939. A method for the preparation of blood filtrates for the determination of sugar. *J. Biol. Chem.* **86**:655.

39. STERN, B. K., and W. E. JENSEN. 1966. Active transport of glucose by suspensions of isolated rat intestinal epithelial cells. *Nature.* **209**:789.

40. STIRLING, C. E. 1967. High-resolution autoradiography of phlorizin-^{3}H in rings of hamster intestine. *J. Cell Biol.* **35**:605.

41. STUMPF, W. E., and L. J. ROTH. 1966. High resolution autoradiography with dry mounted, freeze-dried frozen sections. *J. Histochem. Cytochem.* **14**:274.